# SYMPLIFIED BACKBONE CURVE ESTIMATION METHOD OF UNREINFORCED MASONRY INFILL IN RC FRAME

Kiwoong JIN[1], Ho CHOI[2], Kazuto MATSUKAWA[2] and Yoshiaki NAKANO[3]

[1] Ph.D., Research Assistant Professor, Tokyo Metropolitan University, Tokyo, Japan,
kwjin@tmu.ac.jp
[2] Ph.D., Research Associate, IIS, The University of Tokyo, Tokyo, Japan,
choiho@iis.u-tokyo.ac.jp, mtkw@iis.u-tokyo.ac.jp
[3] Ph.D., Professor, IIS, The University of Tokyo, Tokyo, Japan,
iisnak@iis.u-tokyo.ac.jp

**ABSTRACT**: In this paper, a simplified method to practically estimate the backbone curve of unreinforced concrete block (CB) infill in RC boundary frame is discussed mainly based on the frame geometry and the compressive strength of CB wallette. Representative characteristic points of cracking, maximum, and residual strength of CB infill are employed herein, and their values are proposed to estimate the backbone curve. The estimated backbone curves are found to show good agreement with the test results.

**Key Words**: URM Infill in RC Frame, Diagonal Strut Mechanism, Backbone Curve, FEMA306&356

## INTRODUCTION

In some regions of Asia, Europe, and Latin America where earthquakes frequently occur, serious earthquake damage is commonly found resulting in catastrophic building collapse. Such damaged buildings often have unreinforced masonry (URM) infills, which are considered non-structural elements in the structural design stage, and building engineers have paid less attention to their effects on structural performance although URM infills may interact with boundary RC frames. The evaluation of seismic capacity of URM infills in boundary RC frames is therefore urgently necessary to mitigate earthquake damage for these buildings.

In the previous study (Jin 2012), in-plane cyclic loading tests of one-bay, one-fourth scale RC specimens with unreinforced concrete block (CB) infills for typical school buildings in Korea were carried out, and the measurement plan using 3-axis strain gauges attached on all CB units was employed to experimentally investigate their seismic capacity. The diagonal strut mechanism and lateral load carrying capacity of CB infills were successfully explained based on experiment data using the principal compressive strains of the infills and the strain-stress relationship of CB wallettes.

In this paper, a simplified method to practically estimate the backbone curve of CB infill in RC boundary frame is further discussed mainly based on the frame geometry and the compressive strength of CB wallette.

# EXPERIMENTAL INVESTIGATION OF LATERAL LAOD CARRIED BY CB INFILL IN RC BOUNDARY FRAME

The lateral load carried by CB infill and RC boundary frame is experimentally investigated in the previous study as stated earlier. The experiment outline and the lateral load of CB infill in RC boundary frame are briefly described as follows.

## Experiment Outline

In the previous study (Jin 2012), the test specimens are designed according to the standard design of Korean 4 story school buildings (referred to as "prototype building" shown in figure 1) in the 1980's (The Ministry of Construction and Transportation 2002). From the prototype building, one-fourth scale of two specimens which are infilled frame with rigid beam (IFRB) and infilled frame with flexible beam (IFFB) having an axial load level of their first story are designed as shown in figure 2, and their in-plane cyclic loading tests are carried out. Three-axis strain gauges, which are attached on all CB units (114 units) to estimate the equivalent diagonal strut width and the shear strength of CB infill, are herein the key point of the measurement plan as shown in photo 1.

## Lateral Load Carried by CB Infill in RC boundary Frame

The lateral load carried by RC columns and CB infills in IFRB and IFFB specimens are evaluated by
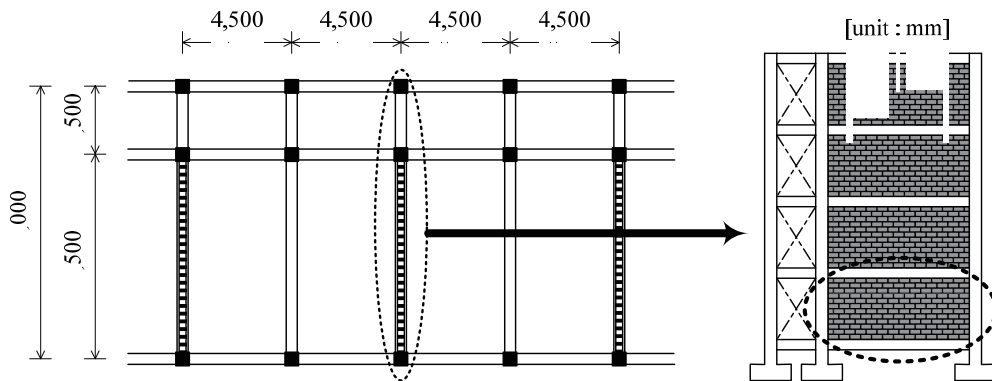


Fig. 1 Standard design of Korean 4 story school buildings in the 1980's
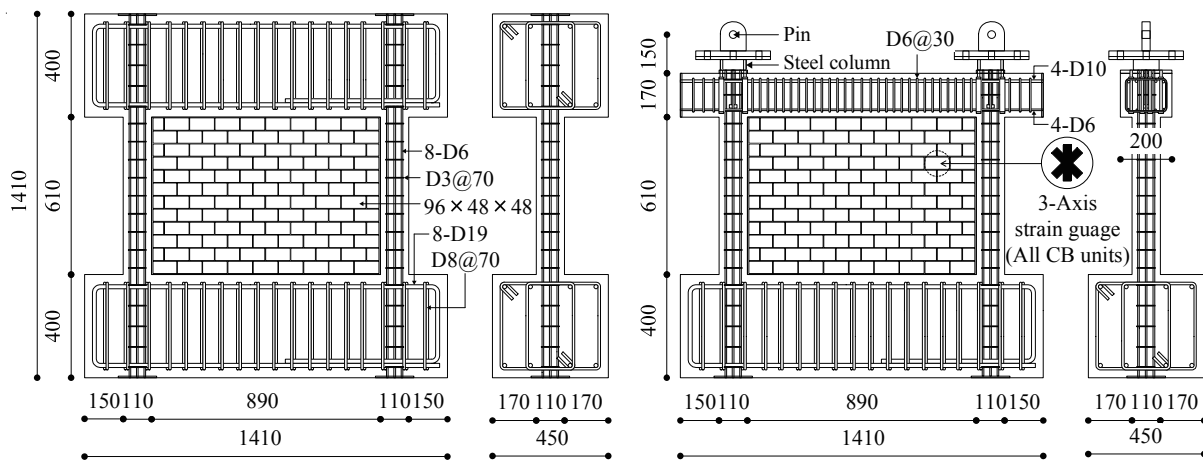


(a) IFRB specimen        (b) IFFB specimen

Fig. 2 Details of specimens (unit : mm)
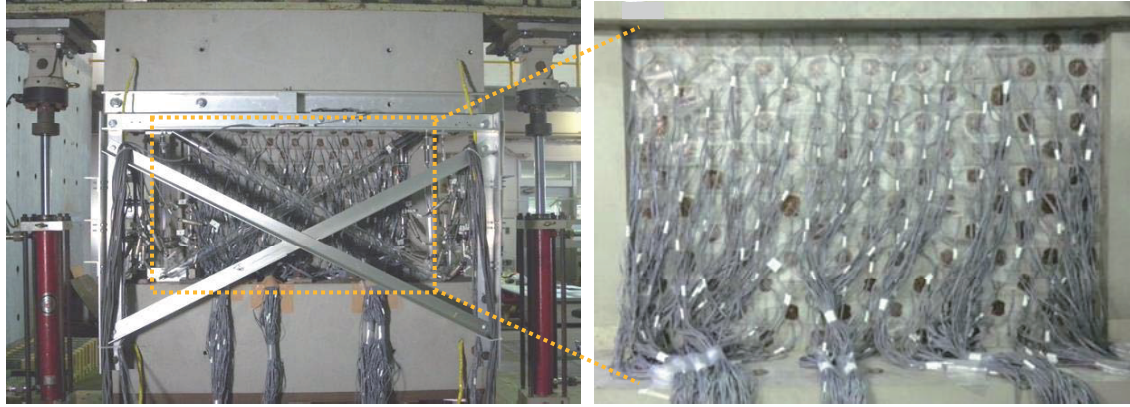
Photo 1 Key point of the measurement plan (Three-axis strain gauges)
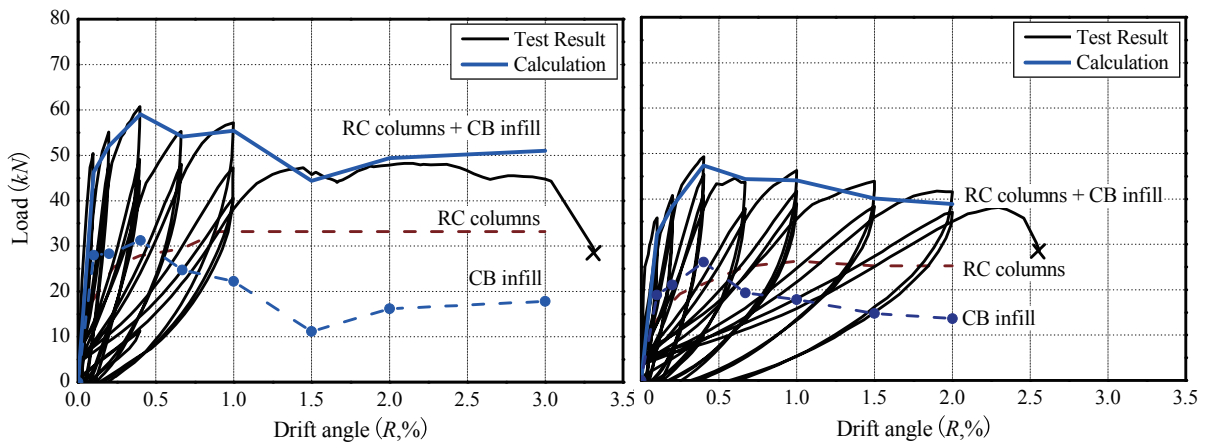


(a) IFRB specimen          (b) IFFB specimen

Fig. 3 Lateral load evaluation of both specimens based on experiment data

using experiment data in the previous study (Jin 2012), and they are compared to the test results as shown in figure 3. In the figure, the lateral load carried by RC columns is calculated from their curvature distribution. On the other hand, that of CB infill is estimated based on the principal compressive strain of diagonal strut acting on the infills and the strain-stress relationship of CB wallettes. As shown in figure 3, the sum of both contribution by RC columns and CB infills well agrees with the overall response recorded in both specimens.

In the next chapter, a simplified method to practically estimate the backbone curve of CB infill in RC boundary frame is further discussed based on the test results.

## PROPOSAL OF SIMPLIFIED BACKBONE CURVE OF CB INFILL

The lateral load carried by CB infills in IFRB and IFFB specimens are again shown in figure 4. As shown in the figure, the stiffness degradation is found before the lateral load reaches its maximum value in both specimens. The load then decreases after the maximum, and it remains almost constant in the larger drift angle. The backbone curve of CB infill in RC boundary frame is therefore simplified as shown in figure 5, and characteristic points of cracking ($R_{cr}$, $V_{w,cr}$), maximum ($R_{max}$, $V_{w,max}$), and residual strength ($R_{res}$, $V_{w,res}$) are employed to represent the curve in this study.

In the next section, a simplified method to practically estimate the backbone curve of CB infill in RC boundary frame shown in figure 5 is proposed mainly based on the frame geometry and the compressive strength of CB wallette.
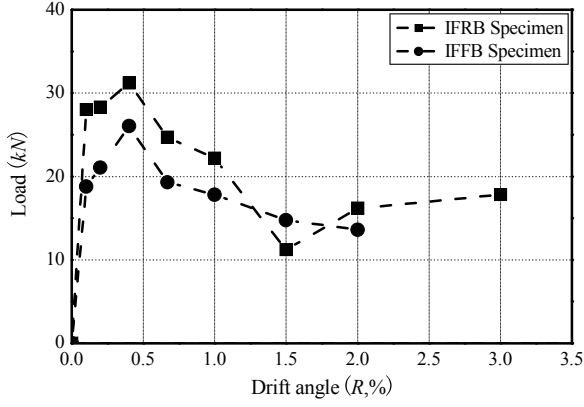
Fig. 4 Lateral load carried by CB infill
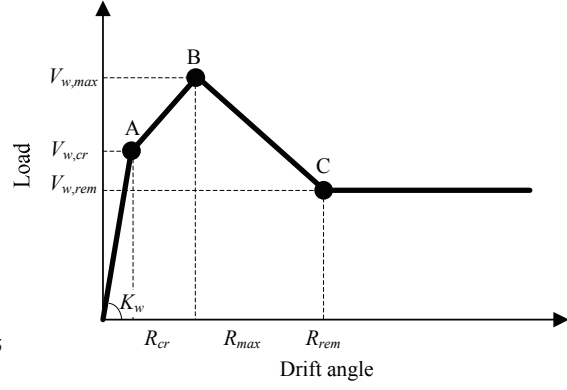


Fig. 5 Simplified backbone curve of CB infill

## Cracking Point on Backbone Curve

### Cracking Strength of CB Infill

The cracking strength $V_{w,cr}$ of CB infill (shown 'A' in figure 5) is first discussed. In the reference (Paulay 1992), the cracking strength $V_{w,cr}$ of CB infill is shown to lie in the range of 50% to 70% of the maximum strength $V_{w,max}$ which will be discussed later. On the other hand, the case where the cracking strength $V_{w,cr}$ exceeds 70% of the maximum strength $V_{w,max}$ is observed in the authors' test results at around the drift angle of 0.1% which corresponds to the cracking point as shown in figure 4. The upper limit shown in the reference (Paulay 1992), which is 70% of the maximum strength $V_{w,max}$, is therefore adopted for the cracking strength $V_{w,cr}$ herein.

### Drift Angle at Cracking Strength

The drift angle $R_{cr}$ ($=V_{w,cr}/K_w$) of cracking strength is calculated from the ratio of cracking strength $V_{w,cr}$ to initial lateral stiffness $K_w$ of CB infill. According to equation (1), the lateral stiffness converted from the axial stiffness of equivalent diagonal strut of CB infill is employed for the initial lateral stiffness $K_w$, which is the same method as found in the reference (FEMA306 1998). In the equation, the Young's modulus $E_m$ of CB infill is obtained from conventional 3-layered CB prism tests (Jin 2012), and the diagonal strut angle $\theta$ is set so that $\tan\theta$ should be the infill height-to-length aspect ratio in the simplified estimation method.

$$K_w = E_m \cdot W_{eq} \cdot \cos^2 \theta \cdot t / l_d \tag{1}$$

in which $E_m$ : Young's modulus of CB infill, $W_{eq}$ : equivalent diagonal strut width, $\theta$ : diagonal strut angle, $t$ : thickness of CB infill, and $l_d$ : diagonal length of CB infill.

In the next section, the equivalent diagonal strut width $W_{eq}$ in equation (1) is discussed, and the effective strut width $W_{e,i}$ and the principal compressive strain $\varepsilon_i$ of CB infill in the diagonal strut, which are necessary to estimate $W_{eq}$, are reviewed from the test results.

### (1) Effective strut width $W_{e,i}$

As stated earlier, the effective strut width $W_{e,i}$ of divided CB infill section $i$, which is a necessary parameter to estimate the equivalent diagonal strut width $W_{eq}$, is reviewed. As is done in the previous study (Jin 2012), the CB infill is first divided to 15 sections ($i$=1 to 15) at an equal interval in the diagonal direction as shown in figure 6, where the principal compressive strains of all CB units obtained from 3-axis strain gauges at the 0.1% drift angle are shown together. The CB units in section $i$ having their angles of the principal compressive strains in the range of 0° through 90° are only considered to calculate the effective strut width $W_{e,i}$, which is defined as the outmost distance of CB units contributing to the strut formation. As can be seen in figure 6, almost all principal strains of CB
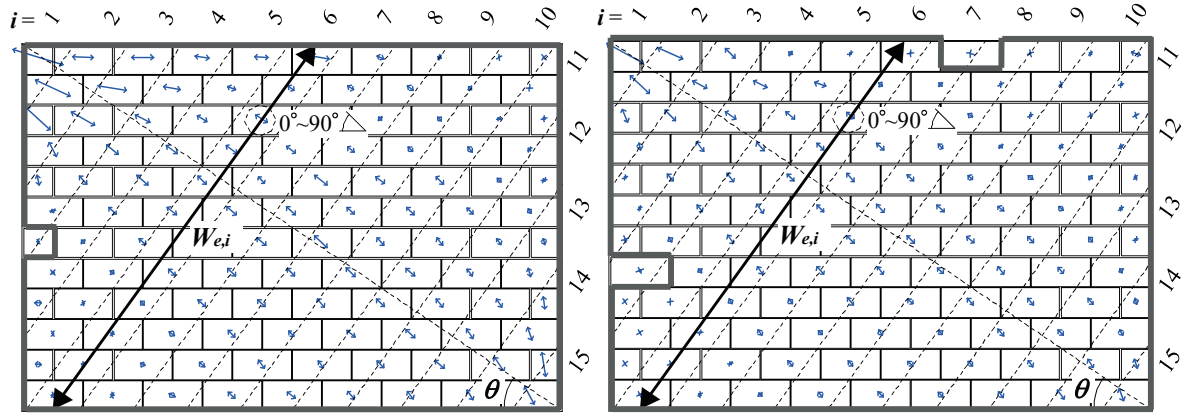
(a) IFRB specimen  (b) IFFB specimen

Fig. 6 CB infill division and principal compressive strain distribution at 0.1% drift angle
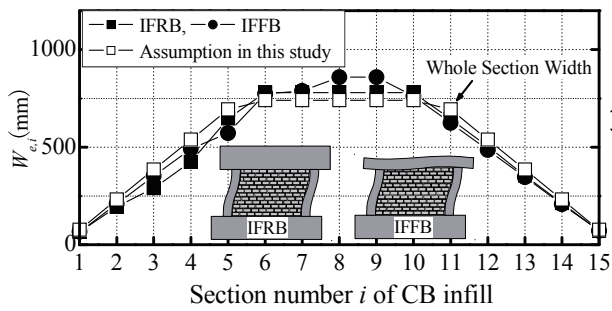


Fig. 7 Effective strut width $W_{e,i}$ at 0.1% drift angle    Fig. 8 Principal comp. strain $\varepsilon_i$ at 0.1% drift angle
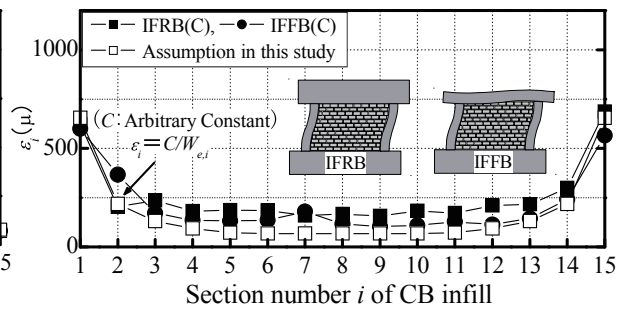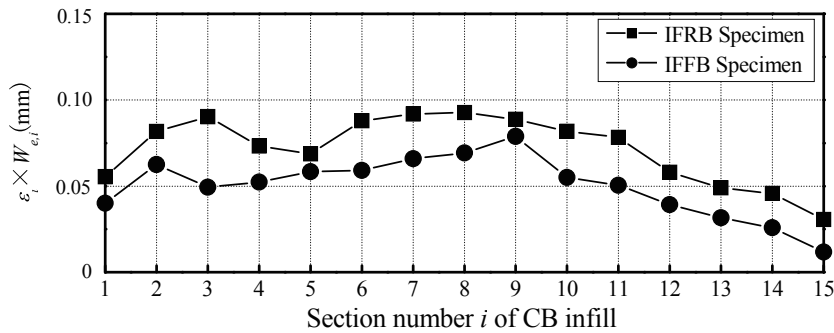


Fig. 9 ($\varepsilon_i \times W_{e,i}$) distribution from the test results at 0.1% drift angle

units have the angles in the range of 0° through 90° (as shown enclosed by a bold line in the figure), and the effective strut width $W_{e,i}$ is simply set the entire edge-to-edge distance of each section determined from the frame geometry. This assumption is plotted with the test results in figure 7, which shows good agreement. It should also be noted that the effective strut width $W_{e,i}$ assumed in this study is slightly lower than the test results in some sections, because the assumed diagonal strut angles are slightly smaller than observed at the drift angle of 0.1% (IFRB:39°, IFFB:45°, Assumption:35°), and $W_{e,i}$ in the tests is therefore longer in some sections than those shown in figure 6.

**(2) *Principal compressive strain $\varepsilon_i$***

The principal compressive strain $\varepsilon_i$ of divided CB infill section $i$, which is another important parameter to estimate the equivalent diagonal strut width $W_{eq}$, is next reviewed. As is done in the previous study

(a) Original Strut   (b) Equivalent Strut
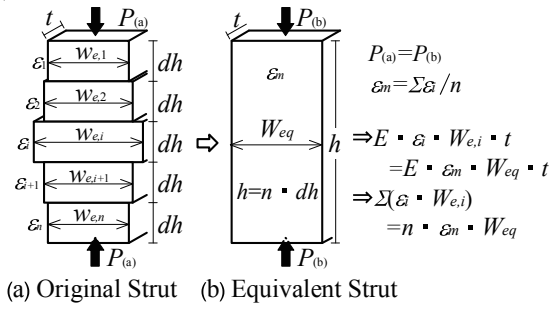
Fig. 10 Equivalent diagonal strut width $W_{eq}$
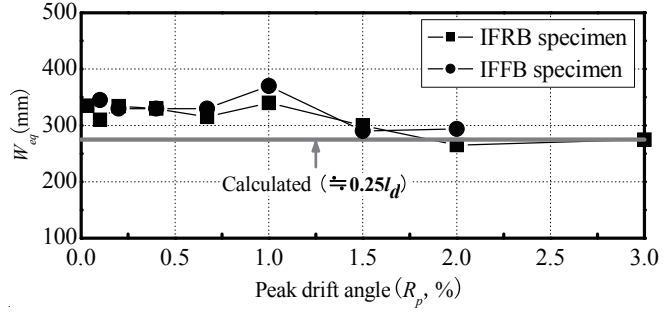


Fig. 11 Comparison of $W_{eq}$ between calculated and test results

(Jin 2012), the principal compressive strains $\varepsilon_i$, which are defined as the average values of principal compressive strains having their angles between 0° and 90° in section $i$, are calculated and shown in figure 8. As can be seen in the figure, the distribution of principal compressive strains $\varepsilon_i$ is roughly inversed shape to that of effective strut width $W_{e,i}$ shown in figure 7. From this observation, the values of $(\varepsilon_i \times W_{e,i})$ in 15 sections are investigated as shown in figure 9, and these values are found roughly constant over all sections in each specimen. The principal compressive strains $\varepsilon_i$ are therefore assumed inversely proportional to the effective strut width $W_{e,i}$, that is, $\varepsilon_i$ equals to $C/W_{e,i}$ where $C$ is the arbitrary constant. The assumed distribution of principal compressive strains $\varepsilon_i$ are also plotted in figure 8, and it well agrees with the test results in both specimens, where the average value of $\varepsilon_1$ and $\varepsilon_{15}$ from the test results are employed to determine the arbitrary constant $C$.

**(3) *Equivalent diagonal strut width $W_{eq}$***
The equivalent diagonal strut width $W_{eq}$ is finally evaluated according to equations (2) and (3), where the same compression force $P$ is assumed to apply to both the original and equivalent strut sections as shown in figure 10. In these equations, the effective strut width $W_{e,i}$ is obtained by the frame geometry, and the principal compressive strain $\varepsilon_i$ is substituted for $C/W_{e,i}$ as explained earlier. The equivalent diagonal strut width $W_{eq}$ is then calculated as 270mm ($\fallingdotseq 0.25l_d$, $l_d$ : diagonal length of CB infill) from equation (3), which can almost approximate the test results as shown in figure 11. It is also found consistent with the value proposed in the reference (Paulay 1992). It should be noted that the equivalent diagonal strut width $W_{eq}$ is also found $0.25l_d$ in the CB infill with different aspect ratio (1.0 and 2.0) from the same evaluation method.

    The the initial stiffness $K_w$ is then calculated from equation (1), and the drift angle $R_{cr}$ ($=V_{w,cr}/K_w$) can be obtained.

$$W_{eq} = \sum_{i=1}^{n}(\varepsilon_i \times W_{e,i})/\sum_{i=1}^{n}\varepsilon_i \tag{2}$$

$$W_{eq} = \sum_{i=1}^{n}(C/W_{e,i} \times W_{e,i})/\sum_{i=1}^{n}(C/W_{e,i})$$
$$= n/\sum_{i=1}^{n}(1/W_{e,i}) \tag{3}$$

in which $\varepsilon_i$ and $W_{e,i}$: principal compressive strain and effective strut width in section $i$, respectively, and $n$ : 15.

**Maximum Strength Point on Backbone Curve**

***Maximum Strength of CB Infill***
The maximum strength $V_{w,max}$ of CB infill on the backbone curve shown in figure 5 (shown 'B') is discussed. The maximum strength $V_{w,max}$ of CB infill is evaluated according to equation (4) as done in the previous study (Jin 2012). In the equation, the equivalent diagonal strut width $W_{eq}$ is set $0.25l_d$ as discussed earlier, and the same angle shown in figure 6 is used for the diagonal strut angle $\theta$.
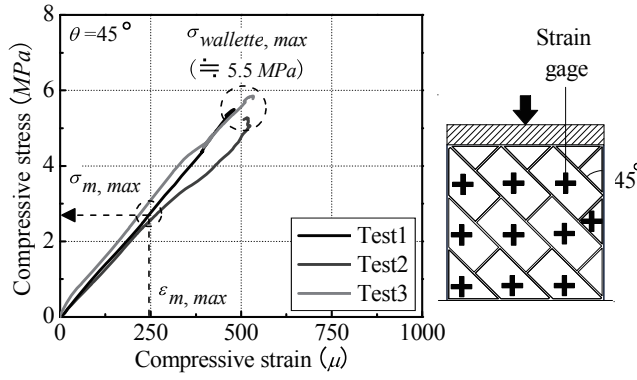
Fig. 12 CB wallettes and stress-strain relation
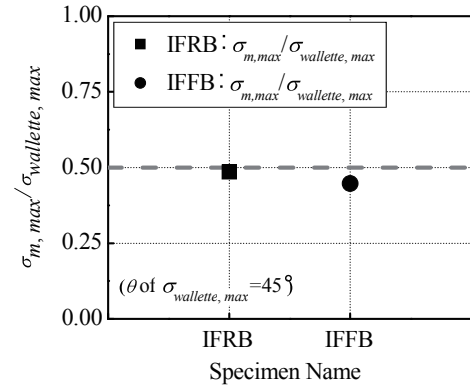


Fig. 13 $\sigma_{m,max}/\sigma_{wallette,max}$ at 0.4% drift angle
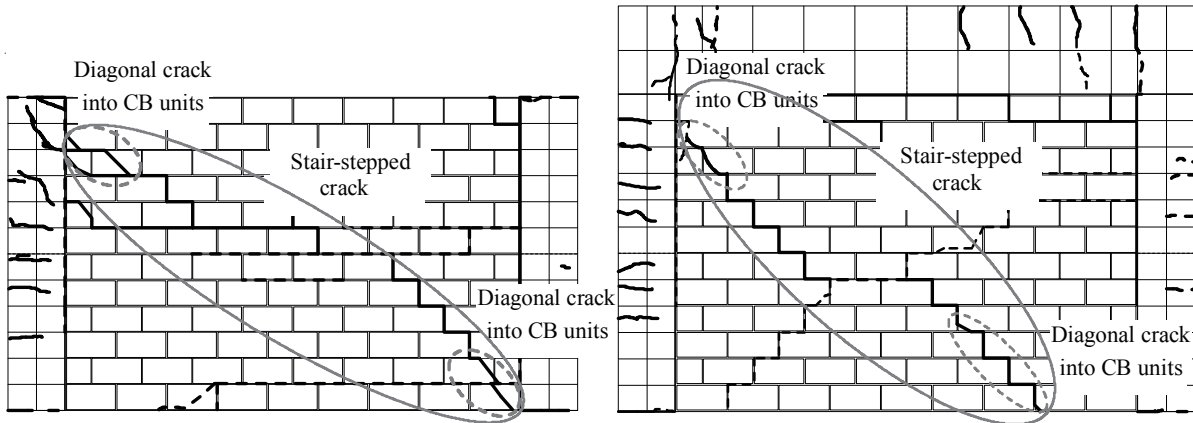


(a) IFRB specimen    (b) IFFB specimen

Fig.14 Damage of CB infill at the drift angle of maximum strength (0.4%)

$$V_{w,\max} = W_{eq} \cdot \sigma_{m,\max} \cdot \cos\theta \cdot t \tag{4}$$

in which $W_{eq}$ : equivalent diagonal strut width, $\sigma_{m,max}$ : maximum value of compressive stress $\sigma_m$ acting on the equivalent diagonal strut at $V_{w,max}$ of CB infill, $\theta$ : diagonal strut angle, and $t$ : thickness of CB infill

The maximum value $\sigma_{m,max}$ of compressive stress $\sigma_m$ acting on the equivalent diagonal strut at $V_{w,max}$ is then required. To obtain the compressive stress $\sigma_m$ acting on the strut, the mean value $\varepsilon_m (=\Sigma\varepsilon_i/15)$ of principal compressive strains $\varepsilon_i$ in 15 sections is first calculated, and the corresponding $\sigma_m$ is evaluated from the stress-strain relations of CB wallette tests. In the wallette tests, three different strut angles of 45°, 37.5°, and 30° are considered but their stress-strain relations and the maximum compressive stress $\sigma_{wallette,max}$ are found almost similar (Jin 2012), and the test result for 45° is exemplified in figure 12 because the strut angles found in both specimens are close to 45° (IFRB:41.3°, IFFB:46.8°). As shown in figure 13, the ratio of $\sigma_{m,max}$ to $\sigma_{wallette,max}$ of CB infill is found approximately 0.5 in both specimens. The compressive stress $\sigma_{m,max}$ acting on the equivalent diagonal strut at the maximum strength $V_{m,max}$ is therefore set 50% of the compressive strength $\sigma_{wallette,max}$ of CB wallette (figure 12).

### Drift Angle at Maximum Strength
In the simplified backbone curve estimation, the damage of CB infill is precisely observed from the test results, and the drift angle $R_{max}$ at maximum strength of CB infill is determined. The damage of CB infill in both specimens at the 0.4% drift angle is shown in figure 14, where the maximum strength of CB infill is recorded. As shown in the figure, stair-stepped cracks fully develop in CB infill along with the diagonal strut, and diagonal cracks into CB units are also found on both ends of the strut. The
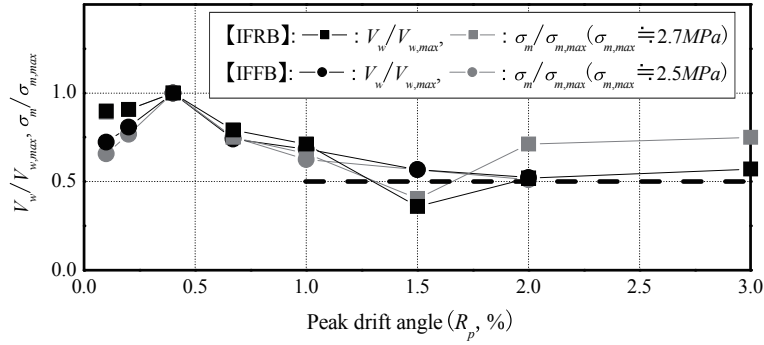
Fig. 15 Variation of $V_w$ and $\sigma_m$ of CB infill
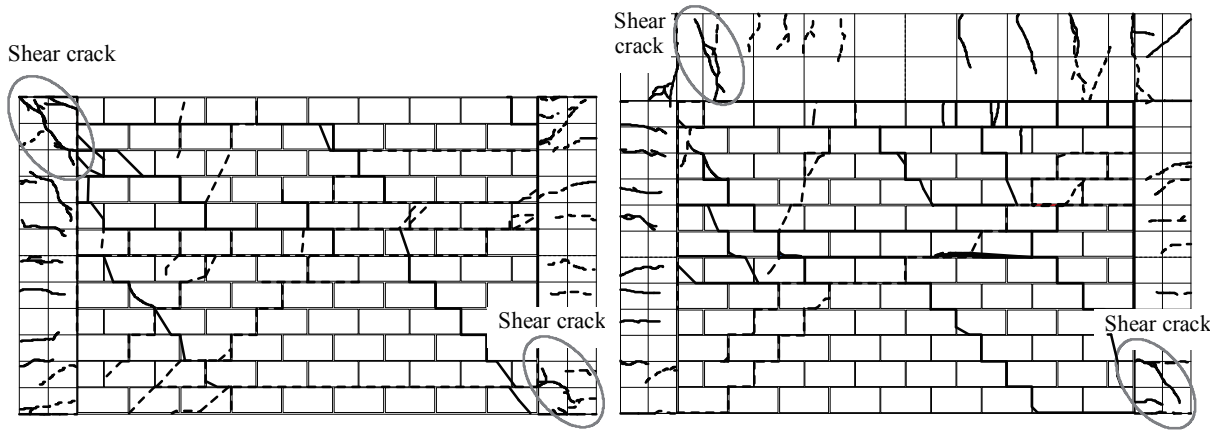


(a) IFRB specimen          (b) IFFB specimen
Fig.16 Damage of CB infill at the drift angle of residual strength (1.0%)

shear strength of CB infill by diagonal strut is therefore assumed to reach the maximum resulting in the full development of stair-stepped crack in the infill, and the drift angle of 0.4% is adopted for the maximum strength. In addition, the reference (FEMA306 1998) explains that these damage of CB infill in RC boundary frame can be usually observed at 0.5% drift angle, which almost agrees with the drift angle $R_{max}$ in this study.

**Residual Strength Point on Backbone Curve**

*Residual Strength of CB Infill*
The residual strength $V_{w,res}$ of CB infill on the backbone curve shown in figure 5 (shown 'C') is next discussed. The residual shear resistance of CB infill is almost 50% of the maximum strength $V_{w,max}$ after the strength degradation as shown in figure 15 (dashed line), where the shear resistance $V_w$ is normalized by $V_{w,max}$, and the half of $V_{w,max}$ is therefore employed for the residual strength $V_{w,res}$ of CB infill. The variation of compressive stress $\sigma_m$ acting on the equivalent diagonal strut, where $\sigma_m$ is also normalized by $\sigma_{m,max}$, is shown together in the figure. As can be seen in the figure, the shear resistance $V_w$ is found mainly dependent on the compressive stress $\sigma_m$, and the reduction of $V_w$ to 50% of $V_{w,max}$ can be attributed to 50% decrease in $\sigma_m$.

*Drift Angle at Residual Strength*
The drift angle $R_{res}$ of residual strength in CB infill is then discussed. As shown in figure 16, it is assumed in this study that the confinement effect of CB infill by RC boundary frame cannot be further expected after the shear cracks almost develops either at the top of tensile column or beam, as well as

at the bottom of compression column, resulting in almost constant shear resistance of CB infill. As shown in the figure, these damage states are observed at the drift angle of 1.0% in both specimens, and it is adopted for the drift angle $R_{res}$.

**Simplified Backbone Curve Estimation Result of CB Infill**

The simplified backbone curve of CB infill in RC boundary frame discussed above are summarized in table 1, and it is compared with the estimation results by the reference (FEMA306 1998, FEMA356 2000) and the test results in both specimens in figure 17. As shown in the figure, the simplified backbone curve proposed in this study shows much better agreement with the test results than FEMA306 and 356.

The overall response evaluated for both specimens is finally demonstrated in figure 18 based on the lateral load carried by RC columns (figure 3) and the simplified backbone curve of CB infill (figure 17) proposed in this study. As can be seen in the figure, the proposed procedure reproduces good agreement with overall response in both specimens.

Table 1 Summary of simplified backbone curve of CB infill in RC boundary frame

| Characteristic points | Damage | Simplified evaluation method |
|---|---|---|
| Cracking strength point ('A' in figure 5) | Separation of CB infill and RC boundary frame, crack initiation of CB infill | ・$V_{w,cr}$ : $0.7V_{w,max}$ ($V_{w,max}$ : cf. Eq.(4)) ・$R_{cr}$ : $V_{w,cr} / K_w$ ($K_w$ : cf. Eq.(1), $W_{eq}$ : $0.25l_d$, $\theta$ : Diagonal angle of infill) |
| Maximum strength point ('B' in figure 5) | Stair-stepped crack fully developed in CB infill in diagonal direction, diagonal cracks into CB units in both ends of stair-stepped crack | ・$V_{w,max}$ : cf. Eq.(4) ($\sigma_{m,max}$ : $0.5\sigma_{wallette,max}$, $W_{eq}$ : $0.25l_d$, $\theta$ : Diagonal angle of infill) ・$R_{max}$ : 0.4% |
| Residual strength point ('C' in figure 5) | Shear crack development in RC boundary frame (either at the top of tensile column or beam and at the bottom of compression column) | ・$V_{w,rem}$ : $0.5V_{w,max}$ ($V_{w,max}$ : cf. Eq.(4)) ・$R_{res}$ : 1.0% |
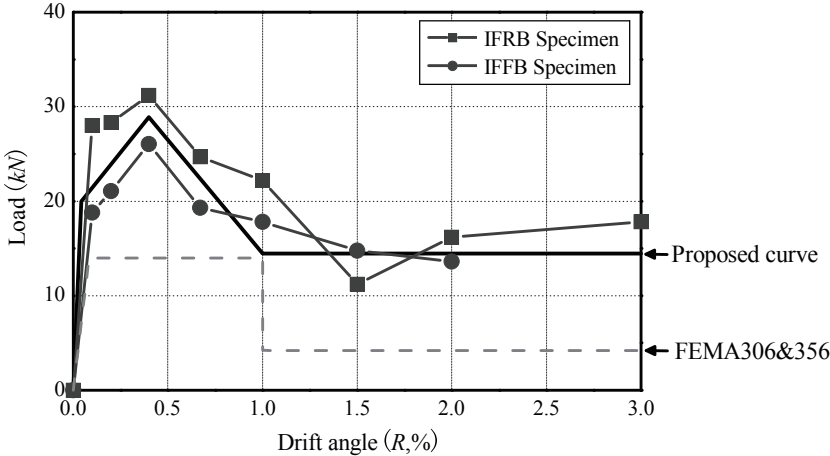


Fig.17 Backbone curve estimation result of CB infill in RC boundary frame
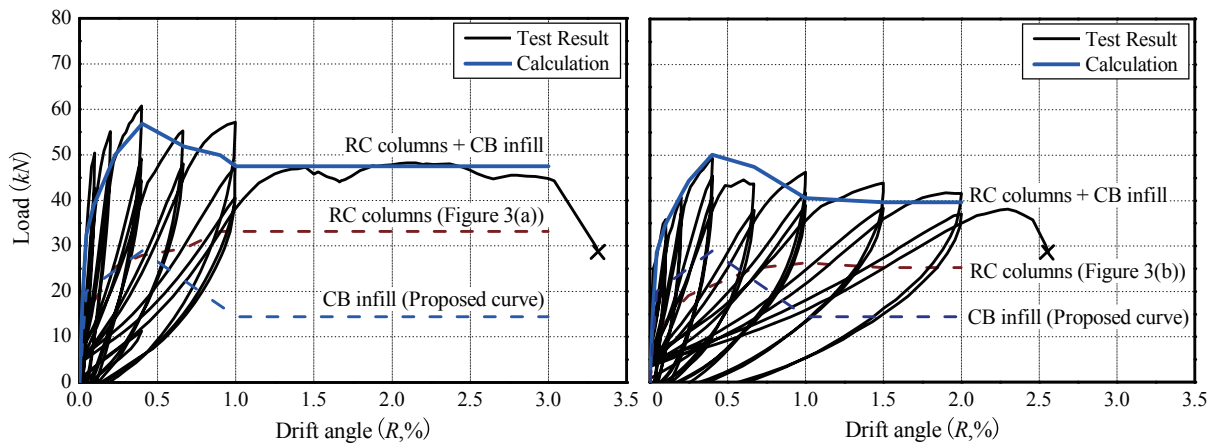
(a) IFRB specimen                  (b) IFFB specimen

Fig. 18 Lateral load evaluation of both specimens by simplified backbone curve of CB infill

## CONCLUSIONS

A simplified method to practically estimate the backbone curve of unreinforced CB infill in RC boundary frame is discussed mainly based on the frame geometry and the compressive strength of CB wallette. The major findings can be summarized as follows.

(1) The backbone curve of CB infill in RC boundary frame can be simply represented by characteristic points of cracking, maximum, and residual strength based on the test results.

(2) The proposed method can evaluate the equivalent diagonal strut width $W_{eq}$ of CB infill based on the frame geometry. It is 25% of diagonal length of CB infill for specimens in this study and found consistent with the previous results proposed by Paulay (2012)

(3) The maximum value of compressive stress acting on the equivalent diagonal strut at the maximum strength of CB infill is 50% of the compressive strength of CB wallette test which is carried out in this study.

(4) The simplified backbone curve proposed in this study shows much better estimation than FEMA306 (1998) and FEMA356 (2000).

## REFERENCES

Jin, K., Choi, H., Takahashi, N., Nakano, Y. (2012). "Seismic Capacity Evaluation of RC Frame with URM Wall Focused on Diagonal Strut Mechanism." Proceedings of 1st International Symposium on Earthquake Engineering, Japan Association for Earthquake Engineering.

The Ministry of Construction and Transportation. (2002). "A study on the seismic evaluation and retrofit of low-rise RC Buildings in Korea (in Korean)".

Paulay, T., Priestley, M.J.N. (1992). "Seismic Design of Reinforced Concrete and Masonry Buildings." JOHN WILEY & SONS, INC.

FEMA 306. (1998). "Evaluation of earthquake damaged concrete and masonry wall buildings." Applied Technology Council (ATC-43 Project).

FEMA 356. (2000). "Prestandard and Commentary for the Seismic Rehabilitation of Buildings."